

## Surface electronic structure of ZrB 2 buffer layers for GaN growth on Si wafers

Yukiko Yamada-Takamura, Fabio Bussolotti, Antoine Fleurence, Sambhunath Bera, and Rainer Friedlein

Citation: [Applied Physics Letters](#) **97**, 073109 (2010); doi: 10.1063/1.3481414

View online: <http://dx.doi.org/10.1063/1.3481414>

View Table of Contents: <http://scitation.aip.org/content/aip/journal/apl/97/7?ver=pdfcov>

Published by the [AIP Publishing](#)

---

### Articles you may be interested in

[Strain states of AlN/GaN-stress mitigating layer and their effect on GaN buffer layer grown by ammonia molecular beam epitaxy on 100-mm Si\(111\)](#)

J. Appl. Phys. **114**, 123503 (2013); 10.1063/1.4822031

[Effect of buffer layer growth temperature on epitaxial GaN films deposited by magnetron sputtering](#)

AIP Conf. Proc. **1447**, 661 (2012); 10.1063/1.4710176

[GaN full-vertical p - i - n rectifiers employing AlGaIn:Si conducting buffer layers on n - Si C substrates](#)

Appl. Phys. Lett. **88**, 193503 (2006); 10.1063/1.2201554

[Buffer controlled GaN nanorods growth on Si\(111\) substrates by plasma-assisted molecular beam epitaxy](#)

J. Vac. Sci. Technol. B **24**, 845 (2006); 10.1116/1.2186342

[Pd growth and subsequent Schottky barrier formation on chemical vapor cleaned p-type GaN surfaces](#)

J. Appl. Phys. **91**, 732 (2002); 10.1063/1.1424060

---

Confidently measure down to 0.01 fA and up to 10 PΩ

Keysight B2980A Series Picoammeters/Electrometers

[View video demo](#)



# Surface electronic structure of $\text{ZrB}_2$ buffer layers for GaN growth on Si wafers

Yukiko Yamada-Takamura,<sup>a)</sup> Fabio Bussolotti,<sup>b)</sup> Antoine Fleurence, Sambhunath Bera,<sup>c)</sup> and Rainer Friedlein

*School of Materials Science and Research Center for Integrated Science, Japan Advanced Institute of Science and Technology (JAIST), 1-1 Asahidai, Nomi, Ishikawa 923-1292 Japan*

(Received 16 April 2010; accepted 31 July 2010; published online 18 August 2010)

The electronic structure of epitaxial, predominantly single-crystalline thin films of zirconium diboride ( $\text{ZrB}_2$ ), a lattice-matching, conductive ceramic to GaN, grown on Si(111) was studied using angle-resolved ultraviolet photoelectron spectroscopy. The existence of Zr-derived surface states dispersing along the  $\bar{\Gamma}$ - $\bar{M}$  direction indicates a metallic character provided by a two-dimensional Zr-layer at the surface. Together with the measured work function, the results demonstrate that the surface electronic properties of such thin  $\text{ZrB}_2(0001)$  buffer layers are comparable to those of the single crystals promising excellent conduction between nitride layers and the substrate in vertical light-emitting diodes on economic substrates. © 2010 American Institute of Physics. [doi:10.1063/1.3481414]

Solid-state lighting using GaN-based light-emitting diodes (LEDs) is believed to contribute significantly to reduction in the world's energy consumption.<sup>1</sup> Conventional LEDs are mostly fabricated on insulating sapphire substrates with electrodes positioned laterally on the same side which leads to current crowding. Additionally, since sapphire is also not a good heat conductor at high temperatures, efficiencies are saturating. Various ways are proposed to accomplish higher efficiencies and higher power, and one of them is the vertical device setup using thermally- and electrically-conductive substrates.

A single crystal of zirconium diboride ( $\text{ZrB}_2$ ) has recently been utilized as a growth template for GaN films demonstrating its superior function as a substrate and an electrode for vertical ultraviolet LEDs.<sup>2,3</sup>  $\text{ZrB}_2$  is a metallic ceramic with a simple crystal structure consisting of alternating, hexagonal close-packed zirconium and honeycomb boron layers with the  $a$ -lattice constant closely matching that of GaN.<sup>2</sup> However, due to the high melting point of  $\text{ZrB}_2$  (3220 °C),<sup>2</sup> it is difficult to grow large single crystals such that the crystal size is currently limited to  $20 \times 20 \text{ mm}^2$ .<sup>3</sup> In addition,  $\text{ZrB}_2$  single crystals have a very high hardness and are easily oxidized such that slicing, polishing, and surface cleaning demand a lot of efforts prohibiting their use as growth templates for the fabrication of economic chips.<sup>4,5</sup>

To overcome these problems,  $\text{ZrB}_2(0001)$  thin films were heteroepitaxially grown on Si(111) allowing the preparation of monopolar, single-crystalline III-nitride films with low defect densities on Si(111) via such buffer layers.<sup>6,7</sup>  $\text{ZrB}_2$  thin films, with thickness as thin as a few tens of nanometer, prepared by chemical vapor method under ultrahigh vacuum (UHV) exhibit resistivity as low as  $20 \mu\Omega \text{ cm}$ ,<sup>8</sup> which

makes the films interesting not just as a lattice-matching buffer layer or as a reflective layer but also as a metallic contact to nitride layer. Obviously, this is a big advantage over insulating AlN, since good electrical conduction between the nitride layer and the Si wafer is required. While a number of studies on  $\text{ZrB}_2$  single crystal surfaces have been reported during the past several years,<sup>4,9,10</sup> the nature of  $\text{ZrB}_2(0001)$  thin film surfaces, in particular the elemental composition of the outermost layer, either Zr or B, and the surface electronic structure governing charge injection into devices, is still a complete mystery. Note that oxide-free thin film surfaces exhibit a  $(2 \times 2)$  reconstruction<sup>7</sup> different from the  $(1 \times 1)$  structure accepted for the clean  $\text{ZrB}_2(0001)$  single crystal surface terminated by a Zr layer.<sup>4</sup> In this study, we demonstrate that surface electronic properties of the  $\text{ZrB}_2$  thin films grown on Si(111) derive from a Zr layer at the surface. Since they are in fact comparable to those of  $\text{ZrB}_2$  single crystals, an excellent vertical conduction at the interface with subsequent GaN layers shall be expected.

$\text{ZrB}_2$  thin films were grown on Si(111) substrates via thermal decomposition of zirconium borohydride [ $\text{Zr}(\text{BH}_4)_4$ ], in a dedicated, custom-built UHV-chemical vapor epitaxy system described in Ref. 8. Natural oxide layers of the Si substrates were removed by first degassing at temperatures below 600 °C for 12 h followed by flash-heating to temperatures higher than 1200 °C as confirmed by the appearance of a reflection high-energy electron diffraction (RHEED) pattern typical for a Si(111)- $(7 \times 7)$  surface. The films were grown by keeping the substrate temperature at 900 °C, and by controlling the  $\text{Zr}(\text{BH}_4)_4$  vapor pressure in the chamber using a leak valve. The borohydride vapor was delivered through a capillary tube with the end positioned a few centimeter away from the substrate surface. Applying a pressure of approximately  $1 \times 10^{-4} \text{ Pa}$  sustains a slow growth rate required for the preparation of epitaxial  $\text{ZrB}_2(0001)$  films.<sup>6</sup> The evolution of the surface during film growth was monitored by RHEED (not shown) and is consistent with low-energy electron diffraction patterns reported previously, employing a similar process.<sup>11</sup> All the films used

<sup>a)</sup> Author to whom correspondence should be addressed. Electronic mail: yukikoyt@jaist.ac.jp.

<sup>b)</sup> Present address: Graduate School of Advanced Integration Science, Chiba University, Chiba, Japan.

<sup>c)</sup> Present address: Laboratoire Interdisciplinaire sur l'Organisation Nanométrique et Supramoléculaire, UMR CEA/CNRS 3299 SIS2M, bât. 125, CEA Saclay F-91191 Gif-sur-Yvette Cedex, France.

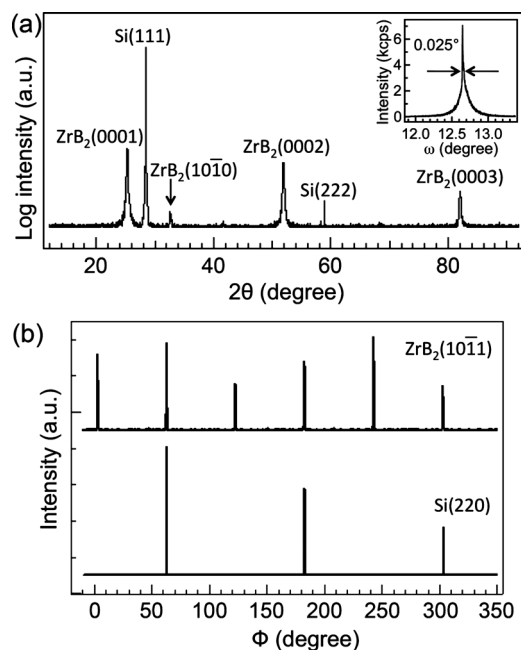


FIG. 1. The results of XRD measurements of a  $\text{ZrB}_2$  thin film on Si(111): (a) ( $\theta$ - $2\theta$ ) scan, and  $\omega$  scan of  $\text{ZrB}_2(0001)$  reflection (inset figure). (b)  $\Phi$  scan of the  $(10\bar{1}1)$  reflection for  $\text{ZrB}_2$  and  $(220)$  reflection for Si.

in this study have shown streaky  $\text{ZrB}_2(0001)$ -( $1 \times 1$ ) RHEED patterns at the end of growth, indicating atomically-flat surfaces, and a transition to a  $\text{ZrB}_2(0001)$ -( $2 \times 2$ ) phase when cooled down to room temperature.<sup>12</sup>

Following the growth, the  $\text{ZrB}_2$  films were taken out from the growth chamber to air for further characterizations. Rutherford backscattering spectrometry determines the film thicknesses to be in the range from 15 to 30 nm depending on the growth conditions and time. The crystal structure of the films was determined by x-ray diffraction (XRD) using a high-resolution thin film XRD system with triple-axis optics. The surface structure was characterized by scanning tunneling microscopy (STM) using a UHV system described in Ref. 12. For any UHV measurements, the oxide layers were removed by heating at 750–800 °C for 12 h.<sup>7</sup> The electronic structure of oxide-free surfaces was studied by angle-resolved ultraviolet photoelectron spectroscopy (ARUPS) in a home-based setup,<sup>13</sup> using unpolarized He I photons ( $h\nu = 21.218$  eV). The total energy and angular resolutions are better than 30 meV and about 0.2°. Before each ARUPS measurement, the high quality of the surface was verified by observing  $\text{ZrB}_2(0001)$ -( $2 \times 2$ ) RHEED patterns identical to those obtained directly following the growth after cooling down the sample to room temperature. The work function was measured from the secondary electron cut-off with the sample biased at -5.0 V.

XRD results are shown in Fig. 1. While the tabulated intensity ratio between  $\text{ZrB}_2(0001)$  and  $\text{ZrB}_2(10\bar{1}0)$  diffractions is 0.45 for randomly oriented crystallites,<sup>14</sup> 112.0 was observed for the film, as shown in Fig. 1(a). Thus, the film is concluded to be nearly perfectly  $c$ -axis oriented. The rocking curve for the  $\text{ZrB}_2(0001)$  reflection is shown in the inset of Fig. 1(a). The full width at half-maximum (FWHM) is as small as 0.025° indicating excellent ordering along the growth direction. The in-plane orientation of the film with respect to the Si substrate was determined by the  $\Phi$  scan of

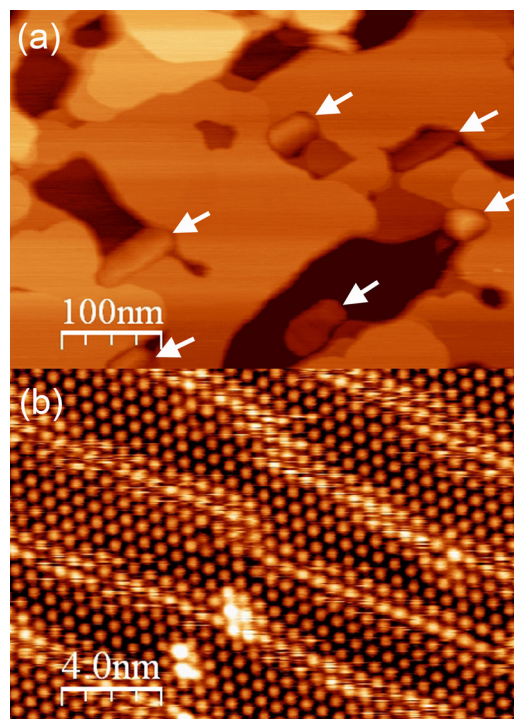


FIG. 2. (Color online) STM images observed for a  $\text{ZrB}_2$  thin film surface after oxide removal. (a) A large-scale image observed with sample bias voltage ( $V_s$ ) of +1 V, and tunneling current ( $I$ ) of 32 pA. White arrows indicate protrusions which are  $\text{ZrB}_2$  crystallites misoriented from the dominant  $\text{ZrB}_2(0001) \parallel \text{Si}(111)$  relation. (b) A high-resolution  $\text{ZrB}_2(0001)$ -( $2 \times 2$ ) image observed at an atomically-flat region with  $V_s = -0.3$  V and  $I = 61$  pA. Domain boundaries show a brighter contrast.

$\text{ZrB}_2(10\bar{1}1)$  and Si(220), and the result is shown in Fig. 1(b). The  $\text{ZrB}_2(10\bar{1}1)$  diffraction reveals a sixfold symmetry which demonstrates that the  $\text{ZrB}_2(0001)$  film has a single in-plane crystal orientation. The comparison of peak positions to those from the Si(220) planes demonstrates in-plane orientation of  $\text{ZrB}_2[10\bar{1}0] \parallel \text{Si}[11\bar{2}]$ . This is consistent with the RHEED observations (not shown), and also with previous studies.<sup>6</sup> The FWHM of the  $\text{ZrB}_2(10\bar{1}1)$  peaks are 0.6° which indicates good crystalline quality. The  $c$ -lattice constant of the film calculated from Fig. 1(a) is  $0.3520 \pm 0.0003$  nm. The film is 0.3% compressed compared to the bulk value of 0.3531 nm,<sup>14</sup> indicating that our film is in a similarly stressed state as the films in Ref. 15 which results in a better lattice matching to GaN.

A large-scale STM image, shown in Fig. 2(a), reveals atomically-flat terraces extending over a few hundred nanometers together with some small protrusions. The terraces are uniformly  $\text{ZrB}_2(0001)$ -( $2 \times 2$ ) reconstructed, as reported previously.<sup>7</sup> A typical atomic-resolution image is shown in Fig. 2(b) providing direct evidence that the terraces derive from  $c$ -axis oriented  $\text{ZrB}_2$  crystals. The areal coverage of the atomically-flat  $\text{ZrB}_2(0001)$  region was estimated to be approximately 80%. Small protrusions are assigned to misoriented  $\text{ZrB}_2$  crystallites<sup>16</sup> that are also observed by XRD shown in Fig. 1(a).

ARUPS spectra taken along the  $\text{ZrB}_2(0001)$   $\bar{\Gamma}$ - $\bar{M}$  direction are shown in Fig. 3 in form of an intensity plot. In this direction, no bulk-derived bands are predicted in the vicinity of the Fermi level allowing a conclusive mapping of the surface electronic structure.<sup>10</sup> At low binding energies, two



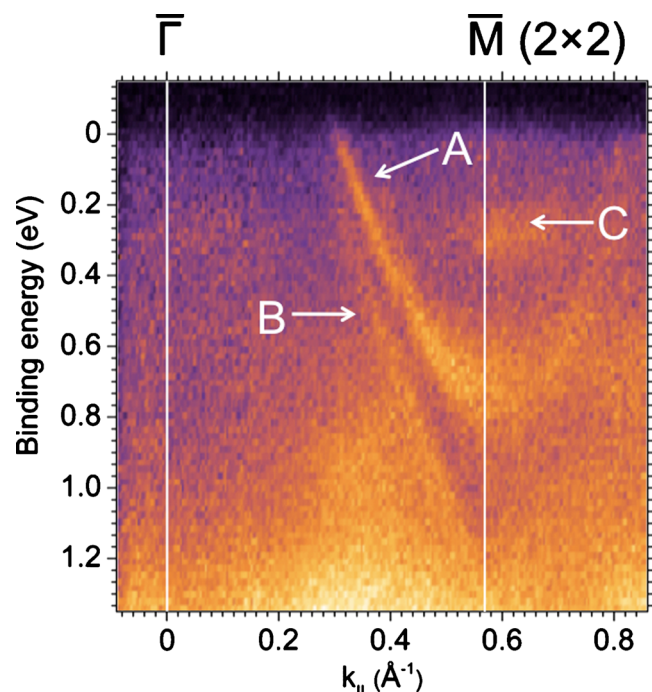


FIG. 3. (Color online) ARUPS spectra of a  $\text{ZrB}_2$  thin film surface along the  $\text{ZrB}_2(0001)$   $\bar{\Gamma}$ - $\bar{M}$  ( $\text{ZrB}_2[10\bar{1}0]$  azimuthal) direction. Strong intensity changes are observed for dispersing Zr-derived surface states, A and B, at the  $\bar{M}$  point of the  $(2\times 2)$ -reconstructed surface. A flat band, denoted C, related to a localized state of adatoms is visible only in the second Brillouin zone along  $\bar{M}$ - $\bar{\Gamma}$ .

features, denoted “A” and “B,” strongly dispersing toward the  $\bar{M}$  point of the  $(2\times 2)$ -reconstructed surface are clearly resolved. These bands cut the Fermi level at intermediate reciprocal momenta proving a metallic character of the surface. While much better resolved over here, similar states have been observed for single crystals<sup>10</sup> and predicted from calculations for a Zr-terminated slab model,<sup>9,10</sup> suggesting a dominant role of Zr  $4d$ ,  $5s$ , and  $5p$  orbitals in the formation of metallic surface states<sup>9</sup> and the presence of a two-dimensional Zr layer at the surface. The pronounced intensity reduction at the  $\bar{M}$  point, located at an in-plane momentum value of  $k_{\parallel}=0.57 \text{ \AA}^{-1}$ , is related to a change in photoelectron emission matrix elements and a strong indication of a switching from positive to negative  $k_{\parallel}$  values at the Brillouin zone boundary.<sup>17</sup>

In the  $\bar{\Gamma}$ - $\bar{K}$  and  $\bar{K}$ - $\bar{M}$  directions, there are predictions for a multitude of narrowly spaced surface and bulk-derived states.<sup>9,10</sup> As predicted for the single crystals, three of the bulk-derived bands are partially filled.<sup>10</sup> These bands are responsible for the conductivity across the film. Fermi surfaces are therefore distinctively different for the bulk and for the outermost surface layer of the thin  $\text{ZrB}_2$  films.

A nondispersing spectral feature, denoted “C” in Fig. 3, at about 0.28 eV has not been observed for single crystals,<sup>9,10</sup> and is therefore related to the  $(2\times 2)$  reconstruction itself. This feature shows enhanced intensity in the second Brillouin zone indicating wave function symmetry of the underlying electronic state different to that of the Zr-derived surface states. It may be conceived that this localized state is fingerprint of adatoms, most likely migrating from the substrate during high temperature treatments. It is important,

however, to emphasize that Zr-derived surface states are robust upon adsorption of these adatoms.

The determination of the work function of freshly prepared surfaces of different samples provided a reproducible value of  $4.61 \pm 0.05 \text{ eV}$ . This value is very close to that of single crystal surfaces,  $4.58 \pm 0.16 \text{ eV}$  measured by Kelvin force microscopy.<sup>3</sup> Since the charge injection properties for the two systems shall therefore be very similar, an excellent vertical conduction between the  $\text{ZrB}_2$  buffer and nitride layers is expected.

In summary, we have demonstrated that despite their difference in the surface reconstruction, epitaxial  $\text{ZrB}_2(0001)$  buffer layers grown on Si(111) have metallic surfaces with electronic properties similar to those of the  $\text{ZrB}_2$  single crystals which would lead to excellent vertical conduction across the interface into subsequent GaN thin films. Thin  $\text{ZrB}_2$  buffer layers will act as heat-resistant bottom contact as well as growth template, reflective layer, and diffusion barrier on silicon wafer. They may therefore well contribute to the realization of economically viable vertical LEDs with high power and high efficiencies.

This work was supported by Special Coordination Funds for Promoting Science and Technology commissioned by MEXT, and also by KAKENHI (Grant No. 19686043). A part of this work was supported by the Murata Science Foundation and the MAZDA Foundation. F.B. acknowledges support from JSPS.

<sup>1</sup>J. M. Phillips, M. E. Coltrin, M. H. Crawford, A. J. Fischer, M. R. Krames, R. Mueller-Mach, G. O. Mueller, Y. Ohno, L. E. S. Rohwer, J. A. Simmons, and J. Y. Tsao, *Laser Photonics Rev.* **1**, 307 (2007).

<sup>2</sup>H. Kinoshita, S. Otani, S. Kamiyama, H. Amano, I. Akasaki, J. Suda, and H. Matsunami, *Jpn. J. Appl. Phys., Part 2* **40**, L1280 (2001).

<sup>3</sup>S. Kamiyama, S. Takamami, Y. Tomida, K. Iida, T. Kawashima, S. Fukui, M. Iwaya, H. Kinoshita, T. Matsuda, T. Yasuda, S. Otani, H. Amano, and I. Akasaki, *Phys. Status Solidi A* **200**, 67 (2003).

<sup>4</sup>T. Aizawa, W. Hayami, and S. Otani, *Phys. Rev. B* **65**, 024303 (2001).

<sup>5</sup>R. Armitage, J. Suda, and T. Kimoto, *Surf. Sci.* **600**, 1439 (2006).

<sup>6</sup>J. Tolle, R. Roucka, I. S. T. Tsong, C. Ritter, P. A. Crozier, A. V. G. Chizmeshya, and J. Kouvetakis, *Appl. Phys. Lett.* **82**, 2398 (2003); J. Tolle, J. Kouvetakis, D.-W. Kim, S. Mahajan, A. Bell, F. A. Ponce, I. S. T. Tsong, M. L. Kottke, and Z. D. Chen, *ibid.* **84**, 3510 (2004).

<sup>7</sup>Y. Yamada-Takamura, Z. T. Wang, Y. Fujikawa, T. Sakurai, Q. K. Xue, J. Tolle, P.-L. Liu, A. V. G. Chizmeshya, J. Kouvetakis, and I. S. T. Tsong, *Phys. Rev. Lett.* **95**, 266105 (2005).

<sup>8</sup>S. Bera, Y. Sumiyoshi, and Y. Yamada-Takamura, *J. Appl. Phys.* **106**, 063531 (2009).

<sup>9</sup>T. Aizawa, S. Suehara, S. Hishita, S. Otani, and M. Arai, *Phys. Rev. B* **71**, 165405 (2005).

<sup>10</sup>S. Kumashiro, H. Tanaka, Y. Kawamata, H. Yanagisawa, K. Momose, G. Nakamura, C. Oshima, and S. Otani, *e-J. Surf. Sci. Nanotechnol.* **4**, 100 (2006).

<sup>11</sup>C. W. Hu, A. V. G. Chizmeshya, J. Tolle, J. Kouvetakis, and I. S. T. Tsong, *J. Cryst. Growth* **267**, 554 (2004).

<sup>12</sup>Z. T. Wang, Y. Yamada-Takamura, Y. Fujikawa, T. Sakurai, Q. K. Xue, J. Tolle, J. Kouvetakis, and I. S. T. Tsong, *J. Appl. Phys.* **100**, 033506 (2006).

<sup>13</sup>F. Bussolotti, S. W. Han, Y. Honda, and R. Friedlein, *Phys. Rev. B* **79**, 245410 (2009).

<sup>14</sup>PDF Number: 00-034-0423, International Centre for Diffraction Data.

<sup>15</sup>R. Roucka, Y. An, A. V. G. Chizmeshya, J. Tolle, J. Kouvetakis, V. R. D’Costa, J. Menendez, and P. Crozier, *Appl. Phys. Lett.* **89**, 242110 (2006).

<sup>16</sup>A. Fleurence and Y. Yamada-Takamura, “Scanning tunneling microscopy investigations of the epitaxial growth of  $\text{ZrB}_2$  on Si(111),” *Phys. Status Solidi* (to be published).

<sup>17</sup>E. Dietz and D. E. Eastman, *Phys. Rev. Lett.* **41**, 1674 (1978).